Supercooling of surface-modified phases

R. Bar-Ziv* and S. A. Safran
Department of Materials and Interfaces, Weizmann Institute of Science, Rehovot 76100, Israel
(Received 8 February 1993; revised manuscript received 29 November 1993)

Recent experiments that probe the effect of alcohol monolayers on the freezing of water are an example of well-characterized surface nucleation, where one has control over the instability by systematic surface modification. We present a simple theory of surface-modified, first-order phase transitions and show how supercooling may in fact be inhibited below a minimal supercooling temperature which is dependent on the macroscopic strength and spatial extent of the surface treatment. The results show that the temperature range where supercooling is possible can indeed vanish for strong enough surface treatments, in qualitative agreement with the experiments.

PACS number(s): 64.60.My, 64.60.Qb, 05.70.Ln, 61.20.Lc

I. INTRODUCTION

A. Overview

Recent experiments [1] use insoluble, well-characterized, surface-active alcohol monolayers to disrupt the supercooling of water and thus induce ice crystal formation. This method of ice nucleation is sensitive to small changes in the properties of the monolayer. These experiments demonstrate that, in contrast to homogeneous nucleation induced by fluctuations [2–5] and heterogeneous nucleation by random defects or impurities, surface nucleation by monolayer additives provides systematic control of the process. Control of the crystallization processes by means of surface additives has technological implications and has been discussed in connection with cloud seeding. In addition to the importation technological implications these experiments may have for the design of new surface-active materials, they raise interesting theoretical questions concerning the effect a well-characterized and controlled surface can have on the stability of the bulk [6].

In this work, we present a phenomenological model of surface-modified, first-order phase transitions and show how supercooling may in fact be inhibited below a minimal supercooling temperature, which is dependent on the strength and spatial extent of the surface treatment. The results show that the temperature range where supercooling is possible can indeed vanish for strong enough surface treatments. In the case of uniform surface modification, presented in Sec. II, we identify a different order-parameter profile which can be induced by even small surface modifications. We show that this state is an intermediate-state (saddle-point) configuration, which can lead to the formation of the equilibrium phase at temperatures higher than those required to cause bulk nucleation.

In the case of surface modification of limited extent, described in Sec. III, the theory also predicts the surface analogy of a critical nucleus size above which supercooling is inhibited. This size is strongly dependent on both the temperature and the strength of the surface treatment and can differ in its dependence on the surface tension and bulk energy from the critical radius in standard nucleation.

B. Experimental motivation

It is a well-known empirical fact that water can be supercooled to temperatures as low as -40 to $-20\,^{\circ}\mathrm{C}$ before transforming into ice [7]. This is in agreement with recent theoretical work on the surface freezing of water, which also indicates that large supercooling should be possible [8]. However, recent experiments by Gavish *et al.* [1] have shown that insoluble, amphiphilic long-chain alcohols, $C_nH_{2n+1}OH$, arranged in two-dimensional crystalline monolayers at the surface of water droplets, disrupt the supercooling of the droplets and thus induce ice crystal formation. This is in contrast to water-soluble alcohols which are effective antifreeze agents. The crystallization was suggested to be induced by a structural match between the two-dimensional monolayer and the attached face of the nucleated ice [1]; a monolayer which was not well matched was a poor ice nucleator.

The minimum supercooling temperature, or effective freezing temperature, was varied from the pure-water value of -20 to nearly $0\,^{\circ}\mathrm{C}$ by changing the microscopic properties of the monolayer. In particular, the effective freezing temperature was correlated with the number of carbon atoms along the chain, n, and its parity. For the odd-numbered chains the freezing temperatures rose from -11 to $0\,^{\circ}\mathrm{C}$ as the chain length increased from $n=17$ to 31, while for the even-numbered chains the freezing temperatures rose for $n<22$ and then leveled off at $8\,^{\circ}\mathrm{C}$ for $n=22$–30. Other long-chain materials (acids), which were not structurally well matched, were used at reference and were poor ice nucleators.

The extent of surface coverage by the monolayer also affected the freezing temperatures. The highest effective freezing temperatures were found for 100% surface coverage. For 75% surface coverage the freezing tempera-

*Present address: Department of Physics of Complex Systems, Weizmann Institute of Science, Rehovot 76100, Israel.

ture fell by 2 °C and for 50% by 8 °C, with respect to 100% coverage [1].

Both lattice mismatch and surface coverage are observed to affect the surface nucleation of ice. Hence, it is not yet clear whether the observed changes of the effective freezing temperature with the hydrocarbon chain length are due to either an increased structural match or an increased strength (i.e., crystallinity) or extent (i.e., island size) of the domains of ordered alcohols.

C. Physical model

In these experiments, microscopic parameters such as the molecular chain length, the lattice mismatch, and the polarity of the molecular head group at the interface, were controlled chemically. Yet the effects induced macroscopic phase transformations. The theory presented here suggests that the chemical modifications used experimentally effectively change the coupling between the monolayer and the liquid and thus change macroscopic parameters (defined below), such as the strength and the spatial extent of the ordering of the liquid at the surface.

To analyze the experiments we note that for a macroscopic system a single monolayer at the liquid-air interface cannot change the thermodynamic freezing temperature of the liquid; it can only affect its stability against nucleation of the solid. The theory presented here considers the stability of the metastable, supercooled state with a spatially varying, scalar order parameter, which is nonzero at the surface and decays to zero away from the surface. In this section we first review the nucleation theory and point out the importance of intermediate (saddle-point) states in destabilizing the system, leading to the equilibrium phase. We then motivate the choice of the order parameter and incorporate the surface effects.

1. Nucleation theory

The classical theory of nucleation, or the droplet model, begins by considering the formation by fluctuations of a droplet of size R of the equilibrium phase embedded in the supercooled phase. The excess free energy of such a droplet is:

$$\Delta F = 4\pi R^2\sigma - \frac{4\pi}{3}R^3\Delta\Gamma \ , \tag{1.1}$$

where σ is the surface tension and $\Delta\Gamma$ is the free-energy difference, per unit volume, between the metastable and stable phases. Equation (1.1) implies that a small droplet will shrink while a large droplet will grow in order to minimize the free energy. The critical droplet size is obtained by maximizing the free energy $(\partial\Delta F/\partial R)(R_c)=0$, from which

$$R_c = \frac{2\sigma}{\Delta\Gamma} \quad \text{and} \quad \Delta F(R_c) = \frac{16}{3}\pi\frac{\sigma^3}{(\Delta\Gamma)^2} \ . \tag{1.2}$$

The probability that a fluctuation corresponding to the critical droplet will occur is proportional to $\exp[-\Delta F(R_c)/k_BT]$ [5].

Nucleation phenomena has been described in a series of papers by Langer [2–4] in terms of a statistical theory of the decay of metastable states which arise in first-order phase transitions. The dynamic evolution of metastable states is given by a phenomenological relaxation equation [5]:

$$\frac{\partial\Psi}{\partial t} = -D\frac{\delta F}{\delta\Psi} \ , \tag{1.3}$$

where $\Psi(\mathbf{r},t)$ is a local, nonconserved order parameter which is zero in the liquid state and nonzero in the solid state, and D is a mobility coefficient. $F\{\Psi\}$ is a free-energy functional which can be modeled quite generally using the Landau-Ginzburg form

$$F\{\Psi\} = \int d\mathbf{r}[f(\Psi)+\tfrac{1}{2}\zeta^2(\nabla\Psi)^2] \ . \tag{1.4}$$

Typically, the bulk free-energy density $f(\Psi)$ has a double-well structure in the coexistence region. The gradient term in Eq. (1.4) accounts for interactions which tend to favor uniform states; such terms are responsible for the positive surface tension of finite systems. The length scale that is characteristic of these gradients is ζ, which is of the order of the molecular size (except near critical points).

The various stable and metastable states are stationary configurations $\{\Psi_s\}$ of Eq. (1.3) which minimize $F\{\Psi\}$; they are thus obtained as solutions of the Euler-Lagrange equation for the minimization of the free energy F:

$$\frac{\delta F}{\delta\Psi} = 0 \ . \tag{1.5}$$

The connection between the metastable or supercooled states and the unstable states that lead to nucleation of the equilibrium phases [2–5] is that a phase transition occurs when a configuration $\{\Psi\}$ near a metastable (or supercooled) state $\{\Psi_{ms}\}$ moves to a more stable minimum of lower free energy. In doing so, the system is most likely to pass (by means of thermal fluctuations or other perturbations) through the lowest intervening saddle point $\{\bar{\Psi}\}$ which is a local maximum (in one direction in phase space) of F that satisfies the Euler-Lagrange equation. Once $\{\Psi\}$ reaches $\{\bar{\Psi}\}$ it is energetically favorable for the system to go "downhill" all the way to the lower minimum. This can be thought of as a steady-state probability current flowing across the saddle point.

This saddle point typically describes a configuration that is almost everywhere similar to the metastable state except for a localized fluctuation of the condensing phase and is an extremum of the free-energy functional. One can expand $F\{\Psi\}$ about $\{\bar{\Psi}\}$:

$$F\{\Psi\} = F\{\bar{\Psi}\} + \frac{1}{2}\int\int d\mathbf{r}\,d\mathbf{r}' M(\mathbf{r},\mathbf{r}')[\Psi(\mathbf{r})-\bar{\Psi}(\mathbf{r})] \times[\Psi(\mathbf{r}')-\bar{\Psi}(\mathbf{r}')]\cdots \ .$$

There is no linear term since $\{\bar{\Psi}\}$ is a stationary point of $F\{\Psi\}$. The operator

$$M(\mathbf{r},\mathbf{r}') = \left[\frac{\delta^2 F}{\delta\Psi(\mathbf{r})\delta\Psi(\mathbf{r}')}\right]_{\{\bar{\Psi}\}} \tag{1.6}$$

has a negative eigenvalue corresponding to one eigendirection along which the free energy diminishes away

from the saddle point, reflecting the fact that $\{\bar{\Psi}\}$ is a local maximum. This eigenvalue is also the initial growth rate of the instability at $\{\bar{\Psi}\}$ [3].

The rate of nucleation is obtained from the steady-state current and is given by [2]

$$I = I_0 e^{-\Delta F/k_B T} \tag{1.7}$$

where the activation barrier is given by

$$\Delta F = F\{\bar{\Psi}\} - F\{\Psi_{\rm ms}\} ,$$

in accordance with the droplet model. I_0 is an inverse time scale which depends on the negative eigenvalue [3,4]; the larger the eigenvalue, the faster the rate.

In summary, the transition from a supercooled state to the equilibrium state is via an intermediate, saddle-point configuration. Although fluctuations are necessary to drive the system to the saddle point, the transition from there to the equilibrium state proceeds in a deterministic manner with no further need for fluctuations. For bulk systems, the saddle-point state is a finite-sized droplet of the equilibrium phase. However, in general, the saddle-point configuration can be any state of the system which is reachable from the supercooled state by fluctuations and which is then unstable to formation of the equilibrium phase. Our results, presented below, identify a different, saddle-point configuration which is not necessarily identical with the equilibrium, ordered phase. This saddle point is driven by the surface modification and is unstable towards formation of the equilibrium.

2. *Order parameter*

We are interested in the propagation of the two-dimensional translational order of the monolayer into the liquid and its eventual destabilizing effects on the metastable liquid state. To highlight the conditions under which the surface treatment can destabilize the liquid, we consider the "best case" of perfect lattice matching between the monolayer and the equilibrium solid. This is consistent with more recent experiments [9] on ice nucleation, which show that two surfaces with identical lattice match, but with different strengths of coupling to the bulk, have very different nucleation temperatures. Even in this best case, our results predict how the strength and extent of the surface ordering can sensitively influence the effective supercooling temperature. The simplification gained by focusing on the best case of complete commensurability of the monolayer and the equilibrium, bulk crystal is that it is only necessary to treat theoretically the spatial variation of the (scalar) amplitude of the crystalline order parameter.

The order parameters which differentiate liquids and solids [10–13] are the fractional density change upon melting, and $\Psi_{\mathbf{G}}$, the Fourier coefficients of the density, where $\mathbf{G}$ are the reciprocal-lattice vectors of the crystalline solid. Each of the crystallinity order parameters $\Psi_{\mathbf{G}}$ is *nonconserved.*

While a complete theory of freezing must focus on both the density and the crystallinity order parameters, we assume that the most dominant effect of the surface is to induce a change in the crystallinity rather than in the density. Therefore, the density order parameter is coupled to the boundary only through the crystallinity order parameters, implying that one can first minimize the free energy with respect to the density and determine it as a function of the local crystallinity (a slave variable). The resulting free energy is then only a function of the crystallinity order parameters, and we consider the simple case of only one Fourier component. A similar procedure has been used by Oxtoby and Haymet [12] and Harrowell and Oxtoby [14] to obtain a local free-energy density as a function of the crystallinity order parameters only, for the case where only one Fourier component is considered. Their free energy, obtained numerically, shows the important features of a metastable state (fluid), a lower-energy equilibrium state (crystal), and an energy barrier. We choose a simple polynomial expansion for this part of the free energy, augmented by a term which accounts for the energy costs of gradients of the order parameter, which is the scalar amplitude of the crystallinity order parameter $|\Psi_{\mathbf{G}}(\mathbf{r})|$, where $\mathbf{G}$ refers to the two-dimensional reciprocal-lattice vectors of the ordered monolayer. We emphasize that our main physical results are independent of the detailed nature of the functional form of the free energy and depend only on the important features noted above.

We therefore consider a free-energy functional $F\{\Psi\}$ as in Eq. (1.4) with a free energy $f(\psi)$ per unit volume which provides a generic model [15] for first-order phase transitions,

$$f(\Psi) = \frac{a(T)}{2}\Psi^2 - \frac{b}{3}\Psi^3 + \frac{c}{4}\Psi^4 . \tag{1.8}$$

Typically, the bulk free-energy density $f(\Psi)$ has a double-well structure in the coexistence region as indicated here, and $a(T)$ is a function which in general can be expanded near the melting temperature as:

$$a(T) = a_0 + a_1(T - T_m) + \cdots , \tag{1.9}$$

with $a_0, a_1 > 0$.

Recent studies of semi-infinite systems with first-order bulk transitions and critical surface phenomena at first-order bulk transitions have used this model [16–18]. The model includes all the distinctive features of first-order transitions: (i) A region of coexistence of two phases in the interval $T \le T_m$, where the phase with $\Psi = 0$ is metastable for $T < T_m$ and the phase with $\Psi = 0$ is stable. When $T = T_m$, the two phases are equally stable, and the transition occurs in equilibrium. (ii) A discontinuous jump of the order parameter at T_m.

3. *Surface effects*

To incorporate the surface effects in the limit of a short-range coupling between the surface and the bulk one can add to the bulk free-energy functional, Eq. (1.4), a surface free energy $f_s(\Psi)$ where,

$$f_s(\Psi) = \int dz\, \delta(z) f_s(\Psi) \equiv f_s(\Psi(z=0)) . \tag{1.10}$$

$\Psi_0 = \Psi(z=0)$ is the surface order parameter and a generic form of the surface free energy f_s is

$f_s(\Psi_0)=-a_1\Psi_0+(a_2/2)\Psi_0^2$ with $a_1,a_2>0$. The first term represents interactions that tend to increase the value of the order parameter at the surface while the second term results in saturation of the surface order parameter (i.e., a free-energy penalty if Ψ_0 is too large). In principle, the equilibrium value of Ψ_0 is found by first calculating the bulk free energy with a fixed value of Ψ_0 as a boundary condition in $\Psi(\mathbf{r})$ and then by minimizing both the surface and bulk free energies with respect to Ψ_0. Thus, one can parametrize the surface by the value of the surface order parameter Ψ_0.

Semi-infinite systems (i.e., systems that are bounded by their surface) which undergo a first-order bulk transition have been considered in the past [16–19]. The main difference between the previous research and the present work is that previous work considered the coupling between the surface and the bulk when the bulk is in its equilibrium stable state and the surface order parameter is unconstrained. The present work considers the effect of a constrained surface on the stability of the bulk when the bulk is metastable rather than stable.

II. INSTABILITIES OF A SURFACE-MODIFIED SUPERCOOLED PHASE

A. Introduction

Motivated by the experiments, we present a model to study the effect a well-characterized surface can have on the stability of a supercooled phase. We first obtain the time-independent solutions of the Euler-Lagrange equation in one dimension for a supercooled bulk with the surface effects of the monolayer entering as a boundary condition (see the previous section). We show that no stationary solutions exist if the surface order parameter becomes too large. Thus, there is a curve in the surface order-parameter–temperature plane, below which there are no metastable states consisting of the bulk, supercooled phase with the monolayer which modifies the surface order parameter. We then perform a linear stability analysis to show that one of the profiles has an instability close to this boundary; we identify the point of instability as the effective freezing point. This curve thus separates the regions where the system can and cannot be supercooled. For the case of uniform surface modification we identify a different saddle-point configuration and identify the relevant fluctuations necessary for nucleation via this saddle point.

The order parameter can be rescaled to give a free-energy functional $F\{\psi\}$, given by Eq. (1.4), where the local free energy Eq. (1.8) of a homogeneous system, $f(\psi)$, is now dimensionless and is given by [15]:

$$f(\psi)=\tfrac{1}{2}\alpha\psi^2-\tfrac{1}{3}\psi^3+\tfrac{1}{4}\psi^4 , \tag{2.1}$$

with

$$\alpha=\frac{2}{9}\frac{a(T)}{a(T_m)} . \tag{2.2}$$

We focus on the temperature range $T<T_m$, where the liquid state with $\psi=0$ is metastable. This corresponds to $\alpha<\frac{2}{9}$. The equilibrium value of the order parameter is given by $\psi_e=\frac{1}{2}(1+\sqrt{1-4\alpha})$. Negative values of ψ are not considered since they are unphysical. In what follows, the spatial coordinate $\mathbf{r}$ is scaled to the microscopic length ζ of this gradient term.

The dynamics of the system is given by Eq. (1.3) in dimensionless form:

$$\frac{\partial\psi}{\partial t}=-\frac{\delta F}{\delta\psi} . \tag{2.3}$$

Stationary profiles, $\psi_s(\mathbf{r})$, i.e., $\partial\psi/\partial t=0$, are solutions of the Euler- Lagrange equation:

$$\left[\frac{\delta F}{\delta\psi}\right]_{\psi_s}=-\nabla^2\psi_s(\mathbf{r})+\frac{\partial f(\psi_s(\mathbf{r}))}{\partial\psi}=0 . \tag{2.4}$$

B. One-dimensional stationary profiles

Consider first a one-dimensional geometry, corresponding to a surface chosen to be at $z=0$, which is completely covered by a monolayer of infinite extent, $L\to\infty$. The interactions of the surface liquid layer with the added monolayer can be complex. In the present model, which assumes short-ranged interactions between the monolayer and the liquid, all of these interactions are lumped into their effect on the value of the order parameter at the surface, $\psi_0=\psi(z=0)$. Experimentally, it is observed that the monolayer is ordered at $T>T_m$, so we consider the case of strong coupling between the monolayer and the fluid surface and take as a boundary condition $\psi(z=0)=\psi_0$, where we consider ψ_0 as a parameter that can be determined from the monolayer-fluid coupling. This choice of the boundary condition can be justified in the case of strong coupling as follows. The general boundary condition has the form $-(\partial\psi/\partial z)_{z=0}+(\partial f_s/\partial\psi)_{z=0}=0$ where $f_s(\psi)$, Eq. (1.10), comes from the coupling of the fluid surface to the monolayer. When this coupling dominates, the gradient term can be neglected and the boundary condition is $\psi(z=0)=\psi_0$, where ψ_0 is the value of ψ which minimizes f_s. Thus, the value of ψ_0 can be varied by changing the properties of the monolayer. Experimentally, the magnitude of ψ_0 is related to the amplitude of the Bragg peak measured in a diffraction experiment, while the coherence length of a surface domain is related to the width of the peak. Thus, in principle, the results may be tested by measuring physical observables.

The Euler-Lagrange equation, Eq. (2.4), is then

$$-\frac{d^2\psi}{dz^2}+\alpha\psi-\psi^2+\psi^3=0 \tag{2.5}$$

from which we construct a first integral:

$$-\frac{1}{2}\left[\frac{d\psi}{dz}\right]^2+f(\psi)=0 . \tag{2.6}$$

The integration constant is zero since away from the surface, as $z\to\infty$, the system is in the homogeneous, supercooled-liquid phase, where both $\psi=0$ and $\partial\psi/\partial z=0$.

In Eq. (2.6) one notices a peculiarity which is due to the competition between the gradient term and the bulk free-energy term. No metastable, time-independent solutions exist if ψ is large enough so that $f(\psi(z))<0$; i.e., for the metastable state with ψ_0 at $z=0$ and $\psi\to 0$ as $z\to\infty$ to be stationary, $f(\psi(z))$ must be non-negative for all z.

In terms of our model, this means that ψ is limited to the range $0<\psi<\psi_M$, where

$$\psi_M=\tfrac{2}{3}(1-\sqrt{1-\tfrac{9}{2}\alpha}) \tag{2.7}$$

is determined by $f(\psi_M)=0$. Thus, in particular, for $T<T_m$, ψ_0 must be smaller than the equilibrium value of the order parameter ψ_e. When $\psi_M<\psi_0<\psi_e$ the stationary solutions of Eq. (2.4) are unphysical and the system is no longer metastable, presumably indicating nucleation of the equilibrium phase since $T<T_m$.

This argument may be reversed and stated in a manner that is more relevant to the experiment. We introduce the minimal supercooling temperature $T^*(\psi_0,L)$, or in dimensionless units $\alpha^*(\psi_0,L)$, which is a function of ψ_0 and the monolayer size L. If the system is supercooled while the surface order parameter ψ_0 is held fixed, then there exists a minimal supercooling temperature, $T^*(\psi_0,L=\infty)<T_m$, below which the system is no longer stationary. Thus, a necessary condition for stationary solutions of Eq. (2.4) is:

$$\alpha>\alpha^*(\psi_0,L=\infty)=\tfrac{2}{3}\psi_0-\tfrac{1}{2}\psi_0^2$$

(as shown in Fig. 1), or

$$T>T^*(\psi_0,L=\infty)\ , \tag{2.8}$$

where

$$T^*(\psi_0,L=\infty)=T_m-\frac{9}{4}\frac{a_0}{a_1}[\psi_0-\psi_M(T_m)]^2\ ,$$

$$0<\psi_0<\psi_M(T_m)\ . \tag{2.9}$$

Integrating Eq. (2.5) we obtain two solutions with $\psi(z=0)=\psi_0$ as boundary condition:

$$\psi_s^{\pm}(z)=\frac{2\alpha\chi^{\pm}e^{-z/\xi}}{(\chi^{\pm}e^{-z/\xi}+\frac{1}{3})^2-\frac{1}{2}\alpha}\ , \tag{2.10}$$

with

$$\chi^{\pm}=\frac{1}{\psi_0}[\alpha-\tfrac{1}{3}\psi_0\pm\sqrt{2\alpha}\sqrt{\tfrac{1}{2}\alpha-\tfrac{1}{3}\psi_0+\tfrac{1}{4}\psi_0^2}]\ . \tag{2.11}$$

The profiles decay over a length scale $\xi=1/\sqrt{\alpha}$. In Eq. (2.11), χ incorporates the effects of ψ_0; $\chi^{\pm}$ have different initial slopes at $z=0$. The first solution $\psi_s^-(z)$, which decreases monotonically from the surface, is obtained by integrating $d\psi/dz=-\sqrt{2f(\psi)}$ in Eq. (2.6). The second solution $\psi_s^+(z)$ has a localized front which extends into the bulk. It can be constructed by integrating first $d\psi/dz=+\sqrt{2f(\psi)}$ out from $z=0$ and $\psi=\psi_0$ to a point $z=z^*$, at which $d\psi/dz=0$ and $\psi_s^+(z^*)=\psi_M$; then $d\psi/dz=-\sqrt{2f(\psi)}$ is integrated to $z\to\infty$. The front is centered at large values of z for small values of ψ_0. When $\psi_0=\psi_M$, $\psi_s^+(z)=\psi_s^-(z)$, and the front is at $z=0$. (See Fig. 2).

In the next section we demonstrate that $\psi_s^-(z)$ is the surface-modified metastable configuration, while $\psi_s^+(z)$ is a higher-free-energy configuration which is an unstable mode. We show that a localized fluctuation of the unstable configuration in a background of the metastable configuration is a different saddle-point configuration that may lead to nucleation of the equilibrium phase. For nucleation of the saddle-point configuration with non-negligible probability, we show that the difference in free energy between the stable and unstable surface-induced states, $\psi_s^-(z)$ and $\psi_s^+(z)$ respectively, must be small. Therefore, the instability associated with this profile is likely to be relevant only when $\psi_0\to\psi_M$, or alternatively when $T\to T^*(\psi_0,L=\infty)$.

C. Linear stability analysis

Equation (2.5) locates local energy minima and saddle-point configurations; the former are metastable while the latter have unstable modes which may grow rather than decay in time and thus lead the transition to the stable

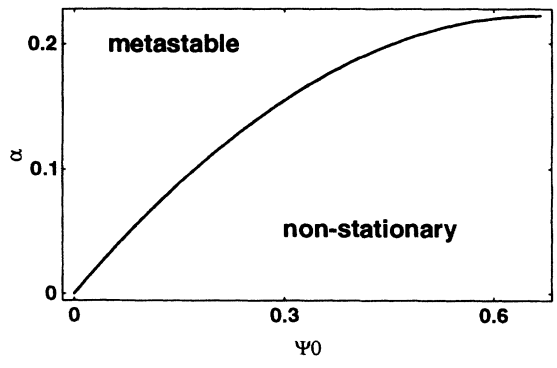

FIG. 1. Critical supercooling temperature $\alpha^*(\psi_0,L=\infty)$ as a function of surface order parameter ψ_0. The region close to the curve (from the metastable region) is where the instability is most likely to occur.

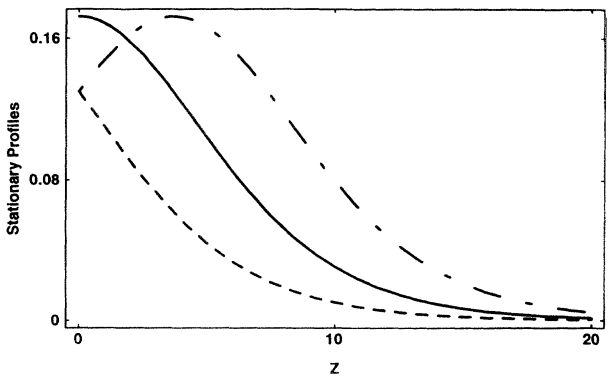

FIG. 2. Stationary profiles obtained with supercooling temperature $\alpha=0.1$. The dashed and dot-dashed curves are $\psi_s^-(z)$ and $\psi_s^+(z)$, respectively ($\psi_0<\psi_M$). The solid curve is $\psi_s^-(z)=\psi_s^+(z)$ ($\psi_0=\psi_M$).

equilibrium phase. We now consider the stability of the stationary solutions $\psi_s^{\pm}(z)$ to small perturbations $\zeta(\mathbf{r},t)$ where $\mathbf{r}=(\rho,z)$ and

$$\zeta(\mathbf{r},t)=\psi(\mathbf{r},t)-\psi_s^{\pm}(z) . \tag{2.12}$$

Letting

$$\zeta(\mathbf{r},t)=e^{i\vec{q}\cdot\vec{\rho}}\phi_q(z)e^{-\Omega_q t}$$

and expanding Eq. (1.3) about $\psi_s^{\pm}(z)$, keeping linear terms in ϕ_q, one finds that Ω_q is determined by the eigenvalue equation [13]:

$$-\phi_{q,zz}+\frac{\partial^2 f(\psi_s^{\pm}(z))}{\partial\psi^2}\phi_q=\omega\phi_q , \tag{2.13}$$

where

$$\omega=\Omega_q-q^2 \tag{2.14}$$

and $\phi_{q,z}=\partial\phi_q/\partial z$.

When $\Omega_q>0$, the perturbation decays in time and the system is still metastable; but when $\Omega_q<0$ the perturbation increases with time, signifying an unstable mode. In addition, the value of the unstable eigenvalue enters into the nucleation rate as explained above. The boundary conditions for Eq. (2.13) are taken to be:

$$\phi_q(z=0)=0 , \tag{2.15a}$$

$$\phi_q \text{ is bounded as } z\to\infty . \tag{2.15b}$$

The first requirement comes from the fact that in Eq. (2.12) $\psi_s(z)$ already obeys the boundary condition set by the surface treatment, $\psi(0)=\psi_0$. Physically this assumes that the surface ordering is constrained and is not affected by the dynamics of the bulk. The second condition comes from the fact that one can make an analogy between unstable modes and bound states of a quantum particle which is localized in a potential well $V^{\pm}(z)$ near the surface [4] where

$$V^{\pm}(z)\equiv\frac{\partial^2 f(\psi_s^{\pm}(z))}{\partial\psi^2}=\alpha-2\psi_s^{\pm}(z)+3[\psi_s^{\pm}(z)]^2 . \tag{2.16}$$

We consider first $q=0$ and discuss finite wave-vector fluctuations in the next section. We first look for $\omega=0$ (marginally stable) modes and then consider $\omega>0$ (stable) and $\omega<0$ (unstable) modes. From Eq. (2.5) one can show that $\phi=d\psi_s/dz$ is a solution of the eigenvalue Eq. (2.13) for $\omega=0$. However, since the surface breaks translational invariance, $d\psi_s/dz$ does not generally satisfy the boundary condition $\phi(0)=0$. In fact, $\phi=d\psi_s/dz$ is a zero eigenmode, consistent with the boundary condition, exactly when $\psi_0=\psi_M$, since then the slope at $z=0$ is exactly zero (see Fig. 2).

The "potentials" of Eq. (2.16) which are associated with the stationary solutions shown in Fig. 2 are plotted in Fig. 3. The solution where $\psi_0=\psi_M(\alpha)$ is marginally stable since its associated potential (the solid curve) has a marginally bound state. However, the lower potential which is associated with ψ_s^+ is shallower and should have a bound state, suggesting that ψ_s^+ is unstable.

The free surface of a liquid (i.e., without a monolayer) does not disrupt supercooling since otherwise the liquid will not supercool. We therefore expect $\psi_s^-(z)$ with $\psi_0\approx 0$ (i.e., the monolayer is at most weakly crystalline) to be stable as this is closest to a free surface configuration. This can be demonstrated from Eq. (2.13) since for small values of ψ we can approximate Eq. (2.13) by

$$-\phi_{zz}+\alpha\phi=\omega\phi . \tag{2.17}$$

The eigenmodes that are consistent with the boundary conditions are all stable and form a continuous spectrum with $\omega>\alpha>0$: $\phi\sim\sin[(\omega-\alpha)z]$. This argument does not hold for $\psi_s^+(z)$ since it has a front extended into the bulk where $\psi\gg 0$.

Since $\phi=d\psi_s/dz$ is a mode with $\omega=0$ only when $\psi_0=\psi_M$, we expect ω to be small when $\psi_0\approx\psi_M$. Regular perturbation theory is inadequate and we thus use the method of singular perturbations [20] to calculate ω perturbatively around $\omega=0$.

Analytic expressions for ω and the corresponding eigenmode are derived in Appendix A. For large z we find:

$$\phi_0(z)\sim e^{-z/\xi+\xi\omega z/2} .$$

For consistency, we require that $\omega<2/\xi^2$. Of the two profiles, the monotonic one, $\psi_s^-(z)$, is linearly stable ($\omega>0$), whereas the profile with the extended front, $\psi_s^+(z)$, is unstable (see Fig. 4). We use these results to plot in Fig. 5 the initial growth, Eq. (2.12), at short times. With increasing time, the perturbation grows into the bulk with $\psi_s^+(z)$ and thus can initiate the phase transition.

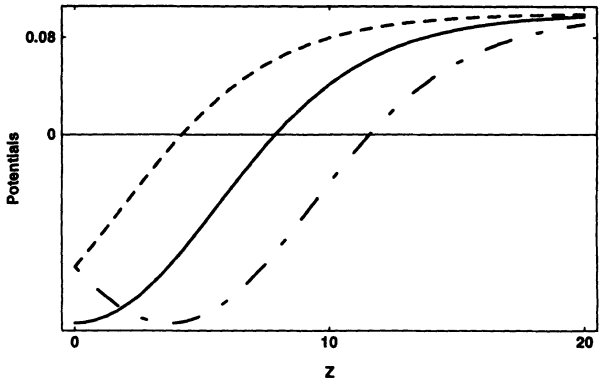

FIG. 3. Potentials corresponding to the stationary profiles obtained with supercooling temperature $\alpha=0.1$. The dashed and dot-dashed curves correspond to $\psi_s^-(z)$ and $\psi_s^+(z)$, respectively (i.e., when $\psi_0<\psi_M$). The solid curve corresponds to $\psi_s^-(z)=\psi_s^+(z)$ (i.e., when $\psi_0=\psi_M$).

D. Nucleation of a surface modified phase

Although unstable, when $\psi_0\ll\psi_M$, or alternatively when $T\gg T^*(\psi_0,\infty)$, the unstable profile labeled by $\psi_s^+(z)$ is unlikely to be induced by surface modification since the front is located far from the surface. Moreover, the unstable state $\psi_s^+(z)$ has a higher free energy than $\psi_s^-(z)$ due to the gradient term in the free energy. Therefore, the probability that the surface will induce a uni-

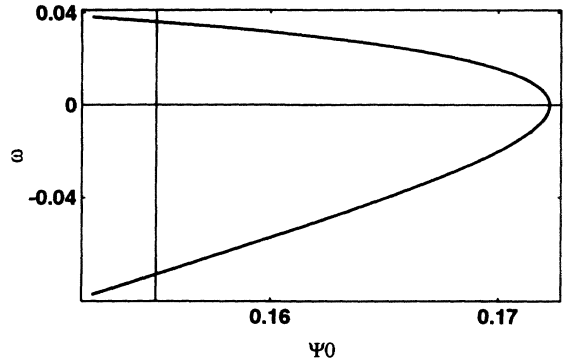

FIG. 4. Plot of ω. The branches of the eigenvalue ω vs ψ_0 corresponding to $\psi_s^-(z)(\omega>0$, stable) and $\psi_s^+(z)(\omega<0$, unstable) for $\alpha=0.1$. $\omega=0$ when $\psi_0=\psi_M$.

form (i.e., infinite in the $\hat{x}$ and $\hat{y}$ directions) configuration corresponding to ψ_s^+ is small unless the free-energy difference between this state and the stable one (ψ_s^-) is small. When $\psi_0\approx\psi_M(\alpha)$, or alternatively when $T\approx T^*(\psi_0, L=\infty)$, the front is near the surface, the two profiles are degenerate. We thus use the relation $\psi_0=\psi_M(\alpha)$, or equivalently the minimal supercooling temperature $T=T^*(\psi_0,\infty)$, to estimate the boundary between metastability and complete instability. Figure 1 shows the dependence of the minimal supercooling temperature $T^*(\psi_0,\infty)$ [in dimensionless units $\alpha^*(\psi_0,\infty)$] as a function of the surface order parameter ψ_0. For a given temperature, surface perturbations that are too "strong" can cause nucleation of the unstable configuration.

This state, ψ_s^+, is a saddle-point configuration as shown by the stability analysis above. Once the system is in that state (e.g., via fluctuations from the stable, surface-induced state, ψ_s^-), the order parameter grows in an unstable manner and the system approaches the equilibrium, ordered phase. Since there is a finite energy difference Δf between the two states for all temperatures $T>T^*(\psi_0,\infty)$, the nucleation barrier for the uniform state is proportional to the sample area A and thus prohibitively high, i.e., the nucleation rate is:

$$I=I_0 e^{-\Delta f A/k_B T} . \tag{2.18}$$

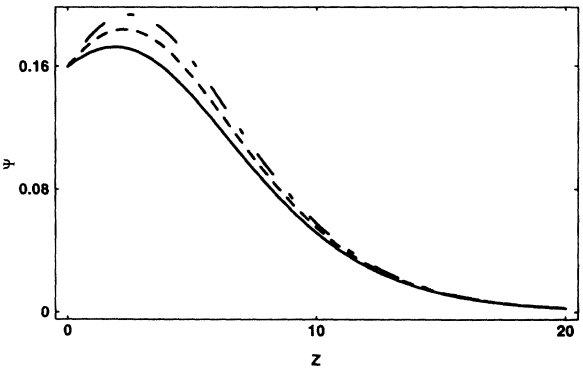

FIG. 5. Plot of the initial growth of instability. The solid curve is $\psi_s^+(z)(\psi_0<\psi_M)$ at $\alpha=0.1$. The dashed and dot-dashed curves are $\psi(z,t)=\psi_s^-(z)+\phi(z,t)$ with $t=0$ and $t=10$, respectively.

Only when $T<T^*(\psi_0,\infty)$ will the one-dimensional state be obtained. However, at temperatures greater than, but close to $T^*(\psi_0,\infty)$, thermal fluctuations can still nucleate finite regions of the unstable phase ψ_s^+ embedded in a phase characterized by the stable profile corresponding to ψ_s^-. This is analogous to classical nucleation but instead of nucleating the equilibrium, ordered phase, the system nucleates an intermediate, but unstable, phase.

Since the energy difference between the two states ψ_s^+ and ψ_s^- can be much smaller than the energy barriers separating the stable state ψ_s^- and the equilibrium state, the nucleation rate for the system to create a small region with a profile given by ψ_s^+ may be orders of magnitude larger than that of the equilibrium state for any given temperature. Of course, the rate is highest at the instability temperature $T^*(\psi_0,\infty)$, where the energy difference between ψ_s^+ and ψ_s^- vanishes. However, there can still be a physically significant rate at somewhat higher temperatures. The nucleation rate is also inversely proportional to the rate of decay of the unstable, saddle-point state as described above.

We can estimate the smallest possible size of such a nucleus, by examining the expression for the decay rate of perturbations of finite wave vector (in the $\hat{x}$ and $\hat{y}$ directions) to the unstable state, ψ_s^+, as described above. This decay rate is always negative (unstable) for uniform or nearly uniform perturbations (i.e., those with small wave vectors q). However, for some critical value of q the perturbations are stable due to the gradient terms in the free energy. In particular, one writes the decay rate as:

$$\Omega_q=-|\omega|+q^2 .$$

We have derived the expression for ω, the $q=0$ eigenvalue, as a function of temperature T and surface order parameter in Appendix A. For $q\gg\sqrt{|\omega|}$ there is no negative eigenvalue and the system is stable. The smallest wave vector below which the system has an unstable mode is thus obtained from the dynamics,

$$q_d=\sqrt{|\omega|} .$$

Hence the smallest possible corresponding surface area of the localized fluctuation is

$$A_d\sim\frac{1}{q_d^2} .$$

For $A\ll A_d$ the system is still stable since $\Omega_q>0$. For $A>A_d$ such fluctuations are unstable and probable only if

$$\frac{\Delta f A_d}{k_B T}\leq 1 .$$

Once the probability of nucleating a finite region with the unstable state ψ_s^+ is finite, the system will then reach the equilibrium ordered state, by decay from the intermediate, unstable, saddle-point configuration.

To estimate the nucleation barrier for fluctuations from the stable state ψ_s^- to the saddle-point configuration ψ_s^+ for a finite region with a critical area A_d, we compare the free-energy difference between these two states,

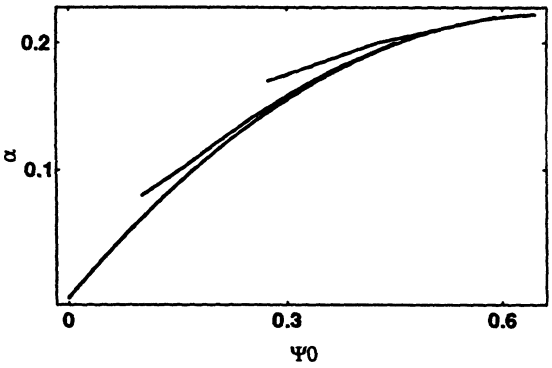

FIG. 6. The middle curve is minimal supercooling temperature $\alpha^*(\psi_0, L=\infty)$ for which $\Delta f A_d/k_B T=0$. The curves above it correspond to $\Delta f A_d/k_B T \approx 0.01$ and 0.05, respectively.

$\Delta f_c(T,\psi_0)$, to the energy of making a critical droplet in homogeneous nucleation which is of order $k_B T$, $\Delta F(R_c)=\frac{16}{3}\pi\sigma^3/(\Delta\Gamma)^2$, where we estimate $\Delta\Gamma=f(\psi_e(\alpha=0.1))$ and $\sigma=\psi_e(T_m)^2/\xi(T_m)$. The lowest curve in Fig. 6 corresponds to the minimal supercooling temperature ($q=0$) for which $\Delta f_c(T,\psi_0)=0$, while the curves above correspond to $\Delta f_c(T,\psi_0)/\Delta F(R_c)=0.01$ and 0.05, respectively, indicating a high probability for unstable finite-wave-vector fluctuations in the vicinity of the $q=0$ curve. Thus, the curve given by $\Delta f_c(T,\psi_0)=0$ is a good guide to the stability of the system.

III. THREE-DIMENSIONAL ORDER-PARAMETER PROFILE

A. Introduction

The previous sections treated the case where the entire surface of the supercooled liquid is modified (e.g., by an added monolayer of size $L\to\infty$). In practice, however, monolayers may be incomplete and consist of domains which may arise due to various reasons: (i) kinetic effects even in monolayer regions which are commensurate with the underlying substrate; (ii) incommensurability effects which define a domain size over which the overlayer and substrate are relatively coherent; or (iii) clusters of oriented dipoles of the molecular head groups. It is not clear yet from experiments which of these different length scales is mostly relevant to the freezing problem and exactly how the domain size enters the problem.

Here we examine the effects of a single, finite domain size on the stability of the system. While a coherent monolayer persisting over the entire surface, inducing an effective surface order parameter ψ_0, leads to an instability of the metastable state if $\psi_0>\psi_M(\alpha)$, or alternatively if $T<T^*(\psi_0,L=\infty)$, we expect that a small enough surface domain will not disrupt metastability even if $\psi_0>\psi_M(\alpha)$. Thus, partial surface coverage by a finite, coherent domain should allow supercooling and stabilize the supercooled liquid with a partially modified surface. For a given supercooling temperature α and a characteristic surface order parameter ψ_0 within the domain, we calculate a critical surface domain size L_c below which the system is metastable, but above which there are no physical stationary solutions, suggesting nucleation of the equilibrium state. This is a two-dimensional analogue to homogeneous nucleation where one needs a critical droplet size to initiate nucleation. However, we note that in the present case the surface order parameter may not be equal to the equilibrium order parameter and may thus vary in magnitude throughout the domain.

An equivalent formulation is that for a given domain size L characterized by a surface order parameter ψ_0 there exists a minimal supercooling temperature $T^*(\psi_0,L)$, which is dependent on both the extent of the domain and its ordering; below $T^*(\psi_0,L)$ further supercooling is inhibited.

B. Critical domain size

We now estimate heuristically the critical domain size L_c above which the monolayer plus supercooled fluid is no longer metastable. We assume an approximate form for the three-dimensional profile within the droplet, which decays in the z direction with a characteristic length λ and in the lateral (x and y directions) with a domain size L.

$$\psi\sim\psi_0\exp\left[-\frac{z}{\lambda}-\frac{\rho^2}{2L^2}\right]. \tag{3.1}$$

λ is a length that will be chosen to minimize the free energy for a given domain size L. Other functional forms can also be considered. We note that L is determined by the response of the (liquid) surface which couples to the surface modification (monolayer). The monolayer has an extent L_m which depends on the internal interactions within the monolayer. For the case of strong coupling to the monolayer, the liquid order parameter at $z=0$ is constrained to have a value which matches the monolayer order parameter over a lateral distance equal to the size of the monolayer, $L=L_m$. However, the free energy f_s [see Eq. (1.10)], which arises from the coupling of the liquid surface to the monolayer, is at its minimum so long as L is at least equal to L_m. Thus, to determine whether $L=L_m$ or $L>L_m$ (i.e., whether the fluid will spontaneously develop a nonzero value of the surface order parameter over a region which is larger than the monolayer extent L_m) we have to examine the bulk and gradient terms in the fluid free energy F. If the free energy of the fluid is increased by an increase in L, then the system will only allow $L=L_m$ (as imposed by the much stronger surface coupling). When the free energy of the fluid is decreased by an increase in L, the system will spontaneously increase, $L>L_m$; this leads to an instability which defines a critical value of $L=L_c$ which represents a maximum in F as a function of L.

To determine this maximal value L_c, we estimate the surface tension from the one-dimensional problem where $\psi_s\sim\psi_0 e^{-z/\xi}$. Thus,

$$\sigma=\int_0^\infty\left[\frac{d\psi_s}{dz}\right]^2 dz\propto\frac{\psi_0^2}{\xi}.$$

With the approximate profile Eq. (3.1), one can show that

the free energy of the system is (neglecting numerical factors)

$$F(\lambda,L)\sim\bar{f}(\psi_0)L^2\lambda+\psi_0^2\lambda+\frac{\psi_0^2L^2}{\lambda} .$$

Here $\bar{f}(\psi_0)$ is an average free-energy density induced by ψ_0 at the surface. We assume that $\bar{f}(\psi_0)<0$ since we consider nucleation of the equilibrium phase. The first term is obtained by integrating over the bulk free energy in Eq. (1.4), the second term comes from the gradient term in z, and the third term results from integrating over the gradients in the x, y directions. Using the definition of the surface tension this free energy is written as

$$F(\lambda,L)\sim[\bar{f}(\psi_0)L^2+\sigma\xi]\lambda+\frac{\sigma L^2\xi}{\lambda} . \tag{3.2}$$

We now minimize F with respect to λ to find

$$\lambda_{\min}^2=\xi\frac{\sigma L^2}{\bar{f}(\psi_0)L^2+\sigma\xi} .$$

Inserting this into $F(\lambda,L)$ yields

$$F_{\min}(L)\sim\{\sigma L^2\xi[\bar{f}(\psi_0)L^2+\sigma\xi]\}^{1/2} . \tag{3.3}$$

Maximizing $F_{\min}(L)$ to find the critical domain size L_c, above which the system is unstable, we find

$$L_c^2\propto\xi\left[\frac{\sigma}{-\bar{f}(\psi_0)}\right] . \tag{3.4}$$

When considering nucleation in the usual approximation, the order parameter is constant and equal to the equilibrium order parameter (i.e., $\psi_0\approx\psi_e$) within the drop (of linear sizes L and λ, as before) and decays over a microscopic length ζ into the liquid. This implies that $\sigma\sim\psi_0^2/\zeta$. Assume

$$\psi\sim\frac{\psi_0}{2}+\frac{\psi_0}{2}\tanh\left[\frac{\rho-\rho_0(z)}{\zeta}\right] , \tag{3.5}$$

where $\rho_0(z)=L(1-z^2/\lambda^2)$ and $\zeta\ll\lambda,L$. One can then show that

$$F(\lambda,L)\sim\bar{f}(\psi_0)L^2\lambda+\sigma\lambda L+\sigma\frac{L^3}{\lambda} ,$$

from which one obtains, by a similar analysis to Eq. (3.3):

$$L_c\propto\frac{\sigma}{|\bar{f}(\psi_0)|} . \tag{3.6}$$

Thus, the fact that the order parameter varies within the droplet induces a dependence of the critical domain size on the surface tension σ and the bulk free energy $f(\psi_0)$, which is different from the usual treatment of nucleation [Eqs. (3.4) and (3.6)].

C. Three-dimensional model

We consider the three-dimensional Euler-Lagrange equation:

$$\frac{\delta F}{\delta\psi}=-\nabla^2\psi+\alpha\psi-\psi^2+\psi^3=0 . \tag{3.7}$$

The order parameter in the $z=0$ plane is modeled by a function $h(x,y)$ which is approximately ψ_0 and decays to zero over a length L. The physical situation of interest is one in which the surface modification is finite but persists over a length which is much larger than the one-dimensional decay length: $L\gg\xi$. In this limit we expect that the surface domain induces a decay of the order parameter which is much slower in the x and y directions than in the z direction. Effectively, the problem reduces to be one dimensional.

The crudest approximation is to neglect the derivatives in x and y and regain the one-dimensional solution with ψ_0 replaced by $h(x,y)$ as surface boundary condition where $h(x,y)\approx\psi_0$ over a length L and decays to zero for $x^2+y^2\gg L^2$. However, this naive approach is limited to systems where $\psi_0<\psi_M(\alpha)$, since the one-dimensional equation has no physical solutions for the local $\psi_0>\psi_M(\alpha)$.

Some insight is gained by noting that terms such as ψ_{xx} scale like $-\psi/L^2$ [21], compared to gradients in the z direction (which are much larger and scale like ψ/ξ^2). "Adding" the terms in ψ_{xx} to the term $\alpha\psi$ indicates that one can heuristically consider the one-dimensional problem with a "redefined" temperature parameter given by $\beta=\alpha+c/L^2$, where c is a positive constant.

Our goal is to approximate the complete Euler-Lagrange Eq. (3.7) by a one-dimensional equation of the form Eq. (2.5) with α replaced by β. Having done so, we then use the argument that the local surface order parameter must be limited by $\psi_0<\psi_M(\beta)$, to find a minimum value of β that is allowed, β_c. The fact that the supercooling temperature α is now coupled to the domain size L by $\beta\approx\alpha+c/L^2$ enables us to obtain a domain size L above which no physical solutions exist in a quasi-one-dimensional equation. We identify this size as the critical size L_c, given as a function of local surface order parameter and supercooling temperature α. Since $\beta>\alpha$ we have $\psi_M(\beta)>\psi_M(\alpha)$ [see Eq. (2.7)] and this restricts the surface order parameter to the range $\psi_M(\alpha)<\psi_0<\psi_M(\beta)$.

In the following, we show how this idea can be used in a perturbation calculation of the three-dimensional profile and L_c [or $T^*(\psi_0,L)$]. We first examine a simple case where $\psi\approx0$ and the solution can be explicitly obtained; we then treat the general case.

D. Three-dimensional profile: small-ψ approximation

We consider the case where $\psi\approx0$ and show how a large length scale emerges in the problem [of course, $\psi\approx0$ means that $\psi<\psi_M(\alpha)$ and that the system is stable for all domain sizes, so we cannot obtain L_c for this case]. We linearize the Euler-Lagrange equation Eq. (3.7):

$$-\nabla^2\psi+\alpha\psi=0 , \tag{3.8}$$

and Fourier transform in x and y:

$$\psi(x,y,z)=\frac{1}{(2\pi)^2}\int\psi(\vec{q},z)e^{i\vec{q}\cdot\vec{\rho}}d^2\vec{q} . \tag{3.9}$$

To model a domain of extent L with a maximum value of order parameter at $\rho=0$ of ψ_0, we use as a simple exam-

ple a Gaussian which allows an analytic treatment:

$$\psi(x,y,z=0)=h(x,y)=\psi_0 e^{-\rho^2/2L^2} . \tag{3.10}$$

(More complex profiles can be treated in a similar manner.) Then, in the limit $L \gg \xi$, one finds

$$\psi(x,y,z)=\frac{\psi_0}{[1+(\xi^2/L^2)(z/\xi)]} \times \exp\left[-\frac{z}{\xi}-\frac{(x^2+y^2)/2L^2}{[1+(\xi^2/L^2)(z/\xi)]}\right] . \tag{3.11}$$

From Eq. (3.11) we see that there are two length scales in the z direction: a fast coordinate z, and a slow coordinate $\bar{z}=(\xi^2/L^2)z$. To introduce this new length scale into the nonlinear problem for arbitrary ψ, we use singular-perturbation theory in a similar manner to the one-dimensional stability analysis.

E. Three-dimensional profile: minimal supercooling temperature

We define the small parameter

$$\epsilon=\frac{\xi}{L} \tag{3.12}$$

and an additional slowly varying z coordinate:

$$\bar{z}=\epsilon^2 z . \tag{3.13}$$

We also scale $\bar{x}=\epsilon x, \bar{y}=\epsilon y$.

The "redefined" temperature β, which differs from α by a term $\sim 1/L^2$, is introduced by an ansatz

$$\beta=\alpha+g(\psi_0,\alpha)\epsilon^2 , \tag{3.14}$$

where the coefficient $g(\psi_0,\alpha)$ is to be determined self consistently. In Appendix B we derive a perturbation expansion and a set of equations for the solution. We obtain a zeroth-order solution Φ_0 in terms of the one-dimensional solution:

$$\Phi_0(\bar{x},\bar{y},z,\bar{z})=\frac{2\beta\chi(\bar{x},\bar{y},\bar{z})e^{-z/\xi_\beta}}{[\chi(\bar{x},\bar{y},\bar{z})e^{-z/\xi_\beta}+\frac{1}{3}]^2-\frac{1}{2}\beta} , \tag{3.15}$$

where $\xi_\beta=1/\sqrt{\beta}$ and $\chi_\pm$ is replaced by $\chi(\bar{x},\bar{y},\bar{z})$. The exact form of $\chi(\bar{x},\bar{y},\bar{z})$ is derived in Appendix B. The result is:

$$\chi(\bar{x},\bar{y},\bar{z})=\frac{\chi_0}{[1+(\xi_\beta/\xi)(\bar{z}/\xi)]} \times \exp\left[\frac{-(\bar{x}^2+\bar{y}^2)/2\xi^2}{[1+(\xi_\beta/\xi)(\bar{z}/\xi)]}+\frac{g(\psi_0,\alpha)\xi_\beta}{2}\bar{z}\right] , \tag{3.16}$$

with

$$\chi_0=\frac{1}{\psi_0}\left[\beta-\tfrac{1}{3}\psi_0-\sqrt{2\beta}\sqrt{\tfrac{1}{2}\beta-\tfrac{1}{3}\psi_0+\tfrac{1}{4}\psi_0^2}\right] . \tag{3.17}$$

Equation (3.15) is our approximate three-dimensional profile (see Fig. 7); it yields a surface order parameter $\Phi_0(x,y,z=0)$ with the property $\Phi_0(\mathbf{r}=\mathbf{0})=\psi_0$, as in the one-dimensional solution Eq. (2.5), which decays asymptotically as $\Phi_0(x,y,z=0)\sim e^{-\rho^2/2L^2}$. In Eq. (3.17) we have chosen the minus sign of Eq. (2.11) corresponding to the stable one-dimensional profile. Thus, for a fixed ψ_0 and L we find that the profile is related to the one-dimensional profile, evaluated at an effective temperature given by $\beta=\alpha+g\xi^2/L^2$. However, this solution is only physical if χ_0 of Eq. (3.17) is real. This restricts $\Phi_0<\psi_M(\beta)$, or $\psi_0=\max[\Phi_0]<\psi_M(\beta)$, where $\psi_M(\beta)=\frac{2}{3}(1-\sqrt{1-\frac{9}{2}\beta})$. This is equivalent to a lower bound on β for fixed ψ_0:

$$\beta>\beta_c=\tfrac{2}{3}\psi_0-\tfrac{1}{2}\psi_0^2\equiv\alpha^*(\psi_0,L=\infty) . \tag{3.18}$$

The coefficient $g(\psi_0,\alpha)$ is given by (Appendix B):

$$g(\psi_0,\alpha)=\frac{4\xi_{\beta_c}}{\xi^2\psi_0^2}\int_0^\infty \Phi_{0,z}^2 dz . \tag{3.19}$$

Here, $\Phi_{0,z}$ is evaluated at $x=y=\bar{z}=0$ with $\psi_0=\psi_M(\beta_c)$ and $\xi_{\beta_c}=1/\sqrt{\beta_c}$. One can identify

$$\sigma\equiv\int_0^\infty \Phi_{0,z}^2 dz \tag{3.20}$$

as the surface tension.

Equations (3.18) and (3.19), together with the definition of β [Eq. (3.14)] and the definition $\alpha=\frac{2}{9}a(T)/a(T_m)$ can be written as:

$$T>T^*(\psi_0,L) , \tag{3.21}$$

where

$$T^*(\psi_0,L)=T^*(\psi_0,\infty)-\left[18\frac{\xi_{\beta_c}}{\psi_0^2}\frac{a_0}{a_1}\right]\frac{\sigma}{L^2} , \quad 0<\psi_0<\psi_M(T_m) \tag{3.22}$$

and $T^*(\psi_0,L=\infty)$ is the one-dimensional critical supercooling temperature (see Sec. II B). Thus, we have shown that a finite size domain implies a minimal supercooling

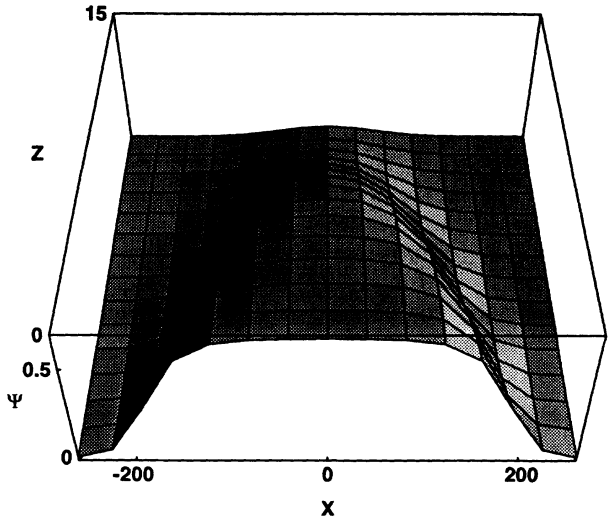

FIG. 7. The shape of Φ_0 from Eq. (3.19) in three dimensions (with $y=0$) at $L=L_c$ with $\psi_0=0.66$ and $\alpha=0.222$.

temperature, which depends both on the domain size L and the surface order parameter ψ_0. The system consisting of the supercooled fluid plus a monolayer is only metastable for temperatures greater than $T^*(\psi_0,L)$. In Fig. 8 we plot the minimal supercooling temperature [in dimensionless units $\alpha^*(\psi_0,L)=\beta_c-g\epsilon^2$] as a function of L for different values of ψ_0. The system may be supercooled above each curve whereas below the curve there are no stationary solutions within our approximation. As expected, for a given L, supercooling is inhibited for large values of the surface order parameter ψ_0. For large L, $T^*(\psi_0,L)$ approaches the one-dimensional minimal supercooling temperature $T^*(\psi_0,L=\infty)$ where $\psi_0=\psi_M(\beta_c)$. [in dimensionless units $\alpha^*(\psi_0,L=\infty)\equiv\beta_c$].

Conditions Eqs. (3.18)–(3.22) may be stated in another way: at a certain supercooling temperature α and a given surface domain characterized by ψ_0 as the maximum value of the surface order parameter, we find a critical domain size L_c above which the system has no stationary solutions:

$$L_c^2=2\xi_{\beta_c}\frac{\sigma}{[-f(\psi_0)]}\ , \tag{3.23}$$

where $f(\psi_0)=\frac{1}{2}\alpha\psi_0^2-\frac{1}{3}\psi_0^3+\frac{1}{4}\psi_0^4<0$ is the bulk free-energy density with $\psi_M(\alpha)<\psi_0<\psi_M(T_m)$. When $\psi_0=\psi_M(\alpha)$, $f(\psi_0)=0$ and $L_c=\infty$; the one-dimensional solution is regained. The physics of this relationship, as well as the connection to the monolayer extent L_m, were described above in Sec. III B, where an expression very similar to Eq. (3.23) was derived in a heuristic manner.

IV. CONCLUSIONS

This work was motivated by recent experiments, performed by Gavish *et al.* [1], that showed that alcohol monolayers at the air-water interface, which are similar in structure to crystalline ice, can prevent supercooling of the water. They showed that the effective freezing points are correlated with the type of alcohol monolayer and its specific properties, in a sensitive and reproducible manner.

The basic idea of the present work is that one can identify the important macroscopic variables in the problem, which are thus affected by the chemical, microscopic changes made in the experiments. We have interpreted these experiments in terms of nucleation theory, focusing on the nucleation of a stable phase from a supercooled phase by systematic and controlled surface modification. This is in contrast to the usual treatments of both homogeneous nucleation, which occurs via thermal fluctuations in the bulk, and heterogeneous nucleation, which takes place at defects or impurities.

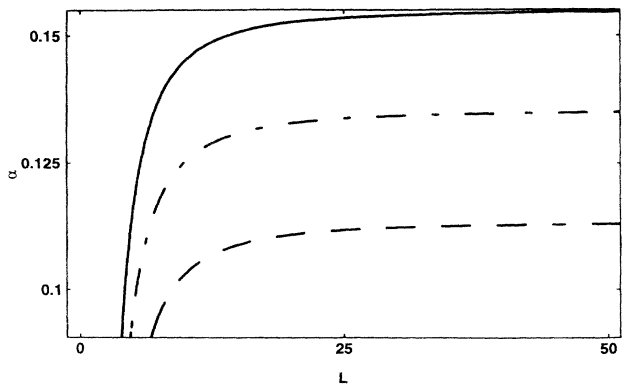

FIG. 8. Critical supercooling temperature $\alpha^*(\psi_0,L)$ vs domain size L for $\psi_0=0.3$ (solid curve), $\psi_0=0.25$ dotted-dashed curve) and $\psi_0=0.2$ (dashed curve).

We showed how a monolayer can act as a mechanism for a dynamic instability, presumably leading to nucleation. As a first approach to this problem, we used a simple Landau-Ginzburg-type model for the phase transition. This model considers the simplest possible coupling (i.e., short range) between the surface and the metastable bulk. In this limit, the monolayer fixes the boundary conditions which are parametrized by (i) the strength of the surface order parameter ψ_0 and (ii) the extent of the ordering, L.

Analysis of the problem for $L\to\infty$ yields a one-dimensional problem and we find two stationary order-parameter profiles which decay away from the surface into the bulk. An important result is that the system cannot be supercooled below a minimal supercooling temperature which is a function of ψ_0. This allows one to draw a boundary separating the regions where the system can and cannot be supercooled. This boundary is in qualitative agreement with the experimental data. A linear stability analysis in the vicinity of the boundary shows that one of the two profiles is a saddle point which may lead to the decay of the metastable state and hence to nucleation. We identified the fluctuations needed to excite this saddle point.

We then considered the problem of a finite surface domain, which necessitates a three-dimensional solution. We find that a small enough domain will not disrupt the supercooled state, while a large enough domain, $L>L_c$, with a strong enough surface order parameter, $\psi_0>\psi_M$, will precipitate the instability. In the limit where the domain size is larger than the bulk decay length of the one-dimensional problem, we find an approximate stationary profile which varies in three dimensions due to the finite domain. Using this approximate profile one can show that the system with finite L may be supercooled below the one-dimensional minimal supercooling temperature, as expected. Furthermore, one can identify a critical domain size above which supercooling is inhibited, which is different from the critical droplet size in homogeneous nucleation, due to the fact that the order parameter varies throughout the surface-induced nucleus.

The experimental work uses local, microscopic changes in the monolayer to change the stability of the bulk, supercooled system. The present theory indicates that those changes can be lumped into their effects on the large-scale properties such as ψ_0 and L and that it is precisely these large-scale properties that determine the effective supercooling temperature.

Finally, we discuss several remaining open questions. First, the use of a single scalar order parameter is appropriate to describe only the magnitude of the order parameter for the freezing transition, but not its phase. To

include the phase, which accounts for the lattice mismatch between the monolayer and the ice lattices, one must consider a complex, multicomponent order parameter. Secondly, this work is limited to short-range interactions between the monolayer and the liquid. It will be interesting to include the effects of long-range forces such as van der Waals interactions. Also, one should look in detail at the physical mechanism behind the domains in the monolayer, perhaps including the effects of dipoles which act as strong constraints at the water-air interface.

ACKNOWLEDGMENTS

The authors acknowledge useful discussions with M. Lahav, L. Leiserowitz, R. Popovitz-Biro, A. Weinstein, K. Binder, R. Lipowsky, and H. Möhwald. The authors also acknowledge support of the U.S.-Israel Binational Science Foundation under Grant No. 90/0009/1 and the Donors of the Petroleum Research Fund, administered by the ACS for partial support of this research.

APPENDIX A: STABILITY ANALYSIS: SINGULAR-PERTURBATION THEORY

In this Appendix we derive an approximate solution for the eigenvalue equation of the one-dimensional stability problem. We denote the stationary solution $\psi_s^+(z)=\psi_s^-(z)$ at which $\psi_0=\psi_M$ by $\eta(z)$. Similarly, χ_m will denote $\chi^+=\chi^-$ in Eq. (2.11), corresponding to the case of $\psi_0=\psi_M$. We define a small parameter

$$\delta=\chi^{\pm}-\chi_m\sim\pm(\psi_M-\psi_0)^{1/2}\ . \tag{A1}$$

From Eq. (2.11) one sees that $\psi_s^-(z)$ and $\psi_s^+(z)$ correspond to values of $\delta<0$ and $\delta>0$, respectively. When $\psi_0\approx\psi_M$, δ is small and we can expand ω in powers of δ:

$$\omega=\omega_1\delta+\omega_2\delta^2+\cdots\ . \tag{A2}$$

There is no constant term since $\omega\to 0$ as $\chi^{\pm}\to\chi_m$. To lowest order in δ, the sign of ω_1 determines which of the two profiles is linearly stable.

We define an additional z coordinate which is slowly varying:

$$\bar{z}=\delta z\ . \tag{A3}$$

Hence, the derivatives of ϕ have contributions from $\bar{z}$:

$$\frac{d^2\phi}{dz^2}=\phi_{zz}+2\delta\phi_{z\bar{z}}+\delta^2\phi_{\bar{z}\bar{z}}\ . \tag{A4}$$

We now write the eigenmode as:

$$\phi(z,\bar{z})=\phi_0(z,\bar{z})+\phi_1(z,\bar{z})\delta+\phi_2(z,\bar{z})\delta^2\cdots\ . \tag{A5}$$

The eigenvalue equation, Eq. (2.13), can be rewritten as

$$-\phi_{zz}+\frac{\partial^2 f(\eta(z))}{\partial\eta^2}\phi=\left[\omega+\frac{\partial^2 f(\eta(z))}{\partial\eta^2}-\frac{\partial^2 f(\psi_s^{\pm}(z))}{\partial\psi^2}\right]\phi\ . \tag{A6}$$

Expanding $\psi_s^{\pm}(z)$ around $\psi_0=\psi_M$ (or $\chi^{\pm}=\chi_m$) is equivalent to

$$\psi_s(z)\approx\eta(z)+(\chi-\chi_m)\left[\frac{\partial\psi_s(z)}{\partial\chi}\right]_{\chi=\chi_m}+\cdots\ .$$

Here, χ denotes either χ^+ or χ^-; $\chi^+=\chi^-=\chi_m$ when $\psi_0=\psi_M$. We thus expand Eq. (A6) in powers of δ. Now,

$$\frac{\partial^2 f(\psi_s^{\pm}(z))}{\partial\psi^2}=\frac{\partial^2 f(\eta(z))}{\partial\eta^2}+\frac{\partial}{\partial\chi_m}\left[\frac{\partial^2 f(\eta(z))}{\partial\eta^2}\right]\delta+\frac{1}{2}\frac{\partial^2}{\partial\chi_m^2}\left[\frac{\partial^2 f(\eta(z))}{\partial\eta^2}\right]\delta^2+\cdots\ . \tag{A7}$$

Since all functions are smooth and regular, the expansion in Eq. (A7) is valid, for all z, provided δ is small enough. Using these definitions we obtain the following equations, to the two lowest orders of δ:

$$-\phi_{0,zz}+\frac{\partial^2 f(\eta(z))}{\partial\eta^2}\phi_0=0\ , \tag{A8}$$

$$-\phi_{1,zz}+\frac{\partial^2 f(\eta(z))}{\partial\eta^2}\phi_1=2\phi_{0,z\bar{z}}+\left[\omega_1-\frac{\partial^3 f(\eta(z))}{\partial\eta^3}\frac{\partial(\eta(z))}{\partial\chi_m}\right]\phi_0\ . \tag{A9}$$

The boundary conditions take the form

$$\phi_0(0)=\phi_1(0)=\cdots=0\ , \tag{A10a}$$

and

$$\phi_n \text{ is finite as } z\to\infty\ . \tag{A10b}$$

The main idea is to use the higher-order terms to find the dependence of ϕ_0 on $\bar{z}$, and the boundary condition to determine ω_1.

Equation (A8) is a linear homogeneous equation which coincides with Eq. (2.13) when $\psi_0=\psi_M$ and $\omega=0$. Its solution is a linear combination of two independent solutions with two "constants of integration," $A(\bar{z})$ and $B(\bar{z})$, which may depend on $\bar{z}$:

$$\phi_0(z,\bar{z})=A(\bar{z})\eta_z(z)+B(\bar{z})\eta_z(z)\int^z\frac{dz'}{[\eta_{z'}(z')]^2}\ . \tag{A11}$$

However, since $\eta(z)\sim e^{-z/\xi}$ for large z, the second solution diverges as $z\to\infty$ and we must choose $B(\bar{z})=0$. The function $A(\bar{z})$ is determined by requiring ϕ_1 to have no irregular behavior as a result of ϕ_0, as described below.

The general solution to Eq. (A9) is given by [20]:

$$\phi_1(z,\bar{z})=C(\bar{z})\eta_z(z)+\int_{z_0}^z K(z,z')G(z',\bar{z})dz'\ , \tag{A12}$$

where [20]

$$K(z,z')=-\eta_z(z)\eta_{z'}(z')\int_z^{z'}\frac{d\bar{z}}{[\eta_{\bar{z}}(\bar{z})]^2}\ , \tag{A13}$$

$$G(z,\bar{z})=2\phi_{0,z\bar{z}}(z,\bar{z})+\left[\omega_1-\frac{\partial^3 f(\eta(z))}{\partial\eta^3}\frac{\partial(\eta(z))}{\partial\chi_m}\right]\phi_0(z,\bar{z})\ ; \tag{A14}$$

z_0 is an arbitrary point in the interval $[0,\infty]$ and we choose $z_0=\infty$. Putting Eq. (A11) into Eq. (A12), with $(\partial^3 f/\partial\eta^3)=-2+6\eta$, we obtain:

$$\phi_1(z,\bar{z})=C(\bar{z})\eta_z(z)-\int_z^\infty K(z,z')\left[2\frac{dA(\bar{z})}{d\bar{z}}\eta_{z'z'}+\left[\omega_1+[2-6\eta(z')]\frac{\partial\eta}{\partial\chi_m}\right]\eta_{z'}(z')A(\bar{z})\right]dz' . \tag{A15}$$

Since $z'>z$ we consider the asymptotic form of the integrand as $z\to\infty$ where,

$$\eta\sim e^{-z/\xi};\quad \frac{\partial\eta}{\partial\chi_m}\sim e^{-z/\xi};$$
$$K(z,z')\sim(e^{(z'-z)/\xi}-e^{(z-z')/\xi}) .$$

To leading order in $e^{-z/\xi}$ the asymptotic form of the integral in Eq. (A15) scales like

$$\sim\int_z^\infty(e^{(z'-z)/\xi}-e^{(z-z')/\xi})\times\left[2\frac{dA(\bar{z})}{d\bar{z}}\frac{1}{\xi^2}-\omega_1A(\bar{z})\frac{1}{\xi}\right]e^{-z'/\xi}dz' . \tag{A16}$$

The first term yields $e^{-z/\xi}\int_z^\infty dz$, which diverges. Hence we choose the constant of integration $A(\bar{z})$ such that

$$2\frac{dA(\bar{z})}{d\bar{z}}-\xi\omega_1A(\bar{z})=0 , \tag{A17}$$

from which we obtain

$$A(\bar{z})=e^{\xi\omega_1\bar{z}/2} . \tag{A18}$$

Thus, with Eq. (A18) we find the zeroth-order eigenmode Eq. (A11):

$$\phi_0(z,\bar{z})=\eta_z(z)e^{\xi\omega_1\bar{z}/2} .$$

We now find the coefficient ω_1 which determines which of the two profiles $\psi_s^\pm$ is linearly stable. To this end we use the boundary condition $\phi_1(0)=0$ in Eq. (A15) which implies:

$$\lim_{z\to0}\eta_z(z)\int_z^\infty\eta_{z'}(z')\int_z^{z'}\frac{d\bar{z}}{[\eta_{\bar{z}}(\bar{z})]^2}\left[\omega_1\xi\eta_{z'z'}+\left[\omega_1+(2-6\eta)\frac{\partial\eta}{\partial\chi_m}\right]\eta_{z'}(z')\right]dz'=0 . \tag{A19}$$

This yields an equation for ω_1 as a function of supercooling temperature α. Since $\eta_z(0)=0$, there are contributions only when the integrand diverges, near $z=0$. For small z we can expand $\eta(z)$ near $z=0$ to second order in z, $\eta(z)\sim a+\frac{1}{2}bz^2$ where there is no linear term because $d\eta/dz=0$ at $z=0$, so that $a=\psi_M$ and $b=(d^2\eta/dz^2)_{z=0}$. In Eq. (A19), ω_1 is determined by the ratio of two integrals. We denote $H(z)=\int dz/\eta_z^2\approx-1/b^2z$, for $z\approx0$ and $H(z)\sim(\xi^3/2)e^{+2z/\xi}$ for $z\to\infty$.

(i) The denominator is:

$$D=\lim_{z\to0}bz\int_z^\infty(\xi\eta_{z'}\eta_{z'z'}+\eta_{z'}^2)[H(z')-H(z)]dz' .$$

Integrating by parts the first term and using the fact that $dH(z')/dz'=1/\eta_{z'}^2$ we find

$$D=\lim_{z\to0}bz\frac{\xi}{2}[\eta_{z'}^2[H(z')-H(z)]]_z^\infty+\lim_{z\to0}bz\int_z^\infty\left[\eta_{z'}^2[H(z')-H(z)]-\frac{\xi}{2}\right]dz' .$$

The first term vanishes. Using $\lim_{z\to0}bzH(z)=-1/b$ we are left with:

$$D=\frac{1}{b}\int_0^\infty\eta_{z'}^2dz'+\lim_{z\to0}bz\int_z^\infty\left[\eta_{z'}^2H(z')-\frac{\xi}{2}\right]dz' .$$

The second integral is finite since the diverging terms in the integrand cancel out due to the fact that $\eta_{z'}^2H(z')\sim\xi/2$ for $z'\to\infty$; so as $z\to0$, the second term does not contribute. Finally, we have for the denominator:

$$D=\frac{1}{b}\int_0^\infty[\eta_z(z)]^2dz . \tag{A20}$$

(ii) The numerator is

$$N=\lim_{z\to0}bz\int_z^\infty\eta_{z'}^2[6\eta(z')-2]\frac{\partial\eta(z')}{\partial\chi_m}[H(z')-H(z)]dz' ,$$

or

$$N=\frac{1}{b}\int_0^\infty(\eta_{z'})^2[6\eta(z')-2]\frac{\partial\eta(z')}{\partial\chi_m}dz'+\lim_{z\to0}bz\int_z^\infty\eta_{z'}^2[6\eta(z')-2]\frac{\partial\eta(z')}{\partial\chi_m}H(z')dz' .$$

The second term is zero in the limit $z\to0$ since the integral has no diverging terms. We thus obtain for the numerator:

$$N=\frac{1}{b}\int_0^\infty[\eta_z(z)]^2[6\eta(z)-2]\frac{\partial\eta(z)}{\partial\chi_m}dz . \tag{A21}$$

This yields

$$\omega_1=\frac{\int_0^\infty[\eta_z(z)]^2[6\eta(z)-2][\partial\eta(z)/\partial\chi_m]dz}{\int_0^\infty[\eta_z(z)]^2dz} . \tag{A22}$$

As a check of consistency we replaced $\phi(z)$ by $\phi_0(z)$ in Eq. (2.13), multiplied by $\phi_0(z)$, and integrated to confirm numerically that

$$\frac{\int\phi_0\{-(d^2\phi_0/dz^2)+[\partial^2f(\psi_s^\pm(z))/\partial\psi^2]\phi_0\}dz}{\int\phi_0^2dz}=\omega\approx\omega_1(\chi^\pm-\chi_m) \tag{A23}$$

holds to a very good approximation for $\chi^\pm\approx\chi_m$.

APPENDIX B: THREE-DIMENSIONAL PROFILE: SINGULAR-PERTURBATION THEORY

In this Appendix we discuss the solutions of Eq. (3.7). The partial derivative in Eq. (3.7) has contributions from z and $\bar{z}$:

$$\frac{\partial^2\psi}{\partial z^2}=\psi_{zz}+2\epsilon^2\psi_{z\bar{z}}+\epsilon^4\psi_{\bar{z}\bar{z}} .$$

Inserting Eqs. (3.13), (3.14) in Eq. (3.7) we obtain

$$-\psi_{zz}-2\epsilon^2\psi_{z\bar{z}}-\epsilon^4\psi_{\bar{z}\bar{z}}-\epsilon^2(\psi_{\bar{x}\bar{x}}+\psi_{\bar{y}\bar{y}}) +\beta\psi-\psi^2+\psi^3=g(\psi_0,\alpha)\epsilon^2 . \quad \text{(B1)}$$

Next, we expand ψ in powers of ϵ:

$$\psi(x,y,z,\bar{z})=\Phi_0+\epsilon\Phi_1+\epsilon^2\Phi_2+\cdots . \quad \text{(B2)}$$

Putting this expansion into Eq. (B1) we obtain the following equations to lowest orders in ϵ:

$$-\Phi_{0,zz}+\beta\Phi_0-\Phi_0^2+\Phi_0^3=0 ; \quad \text{(B3)}$$

$$-\Phi_{1,zz}+(\beta-2\Phi_0+3\Phi_0^2)\Phi_1=0 ; \quad \text{(B4)}$$

$$-\Phi_{2,zz}+(\beta-2\Phi_0+3\Phi_0^2)\Phi_2 =\Phi_{0,\bar{x}\bar{x}}+\Phi_{0,\bar{y}\bar{y}}+2\Phi_{0,z\bar{z}}+g(\psi_0,\alpha)\Phi_0 . \quad \text{(B5)}$$

These equations must be solved subject to the boundary conditions:

$$\Phi_0(z=0)=h(x,y) ; \quad \text{(B6a)}$$

$$\Phi_1(z=0)=\Phi_2(z=0)=\cdots=0 . \quad \text{(B6b)}$$

For consistency of the perturbation expansion we require that each successive approximation will have no unbound terms. We use these equations to solve for both the order parameter profile and the critical size L_c.

Equation (B3) is the quasi-one-dimensional equation which coincides with the one-dimensional Euler-Lagrange Eq. (2.5) when $\epsilon=0$. Its solution can be written as Eq. (3.15), where $\xi_\beta=1/\sqrt{\beta}$. Equation (B4) is a linear equation and we can choose Φ_1 to equal zero. The exact form of $\chi(\bar{x},\bar{y},\bar{z})$ is determined by requiring that Φ_2 have no irregular behavior as a result of the zeroth-order solution Φ_0.

The solution to Eq. (B5), which is an ordinary linear differential equation, is obtained by integrating with respect to z, holding $\bar{x}$, $\bar{y}$, and $\bar{z}$ fixed. The general solution is given by [20]:

$$\Phi_2(\bar{x},\bar{y},z,\bar{z})=A(\bar{x},\bar{y},\bar{z})\Phi_{0,z} +\int_{z_0=\infty}^{z}K(z,z')G(z')dz' . \quad \text{(B7)}$$

We have discarded in Eq. (B7) a solution which is unbound (see Appendix A). As in Appendix A:

$$K(z,z')=-\Phi_{0,z}\Phi_{0,z'}\int_z^{z'}\frac{d\bar{z}}{(\Phi_{0,\bar{z}})^2} \quad \text{(B8)}$$

and

$$G(z')=\Phi_{0,\bar{x}\bar{x}}(z')+\Phi_{0,\bar{y}\bar{y}}(z')+2\Phi_{0,z\bar{z}}(z') +g(\psi_0,\alpha)\Phi_0(z') . \quad \text{(B9)}$$

The dependence of G and K on $\bar{x},\bar{y},\bar{z}$ has been omitted for brevity. Using Eq. (3.15) for Φ_0 and the chain rule we obtain for the derivatives in G:

$$\Phi_{0,\bar{x}\bar{x}}=\xi_\beta\left[\frac{\chi_{\bar{x}}^2}{\chi^2}(\Phi_{0,z}+\Phi_{0,zz}\xi_\beta)-\frac{\chi_{\bar{x}\bar{x}}}{\chi}\Phi_{0,z}\right] , \quad \text{(B10)}$$

and a similar expression for $\Phi_{0,\bar{y}\bar{y}}$. Also,

$$\Phi_{0,z\bar{z}}=-\xi_\beta\Phi_{0,zz}\frac{\chi_{\bar{z}}}{\chi} . \quad \text{(B11)}$$

Putting this back in Eq. (B7) we have:

$$\Phi_2(\bar{x},\bar{y},z,\bar{z})=A(\bar{x},\bar{y},\bar{z})\Phi_{0,z}+\xi_\beta\int_\infty^z K(z,z')\left[-2\Phi_{0,z'z'}\frac{\chi_{\bar{z}}}{\chi}-\left[\frac{\chi_{\bar{x}\bar{x}}}{\chi}+\frac{\chi_{\bar{y}\bar{y}}}{\chi}\right]\Phi_{0,z'}+\left[\frac{\chi_{\bar{x}}^2}{\chi^2}+\frac{\chi_{\bar{y}}^2}{\chi^2}\right](\Phi_{0,z'}+\Phi_{0,z'z'}\xi_\beta) +\frac{1}{\xi_\beta}g(\psi_0,\alpha)\Phi_0\right]dz' . \quad \text{(B12)}$$

As in Appendix A for the stability analysis we now look at the asymptotic behavior of the integral, for large values of z:

$$\Phi_0\sim e^{-z/\xi_\beta};\quad K(z,z')\sim(e^{(z'-z)/\xi_\beta}-e^{(z-z')/\xi_\beta}) .$$

Hence, to leading order in e^{-z/ξ_β} the asymptotic form of the integral is

$$\int_z^\infty(e^{(z'-z)/\xi_\beta}-e^{(x-z')/\xi_\beta})\left[-\frac{2}{\xi_\beta^2}\frac{\chi_{\bar{z}}}{\chi_\beta}+\frac{1}{\xi}\left[\frac{\chi_{\bar{x}\bar{x}}}{\chi}+\frac{\chi_{\bar{y}\bar{y}}}{\chi}\right]+\frac{1}{\xi_\beta}g(\psi_0,\alpha)\right]e^{-z'/\xi_\beta}dz' . \quad \text{(B13)}$$

The third term in the square brackets of Eq. (B12) is missing in Eq. (B13) since $\Phi_{0,z'}\sim-\Phi_{0,z'z'}\xi_\beta$ asymptotically. The integral will diverge unless we set:

$$\frac{2}{\xi_\beta}\chi_{\bar{z}}-\chi_{\bar{z}\bar{z}}-\chi_{\bar{y}\bar{y}}-g(\psi_0,\alpha)\chi=0 . \quad \text{(B14)}$$

This equation determines $\chi(\bar{x},\bar{y},\bar{z})$. Equation (B14) is solved by defining

$$\eta=e^{-a\bar{z}}\chi , \quad \text{(B15)}$$

where $a=g(\psi_0,\alpha)\xi_\beta/2$. This yields the differential equation:

$$\eta_{\bar{y}\bar{y}}+\eta_{\bar{x}\bar{x}}-\frac{2}{\xi_\beta}\eta_{\bar{z}}=0\ . \tag{B16}$$

The boundary condition at $\bar{z}=0$ is chosen for convenience to have the form

$$\eta(\bar{x},\bar{y},0)=\chi(\bar{x},\bar{y},0)=\chi_0\exp\left[-\frac{x^2+y^2}{2L^2}\right]$$
$$=\chi_0\exp\left[-\frac{\bar{x}^2+\bar{y}^2}{2\xi^2}\right]\ .$$

This particular choice for the boundary condition of χ is made in order to obtain a simple analytic solution of Eq. (B14) and will yield only asymptotically $\Phi_0(x,y,z=0)\sim\exp[-(x^2+y^2)/2L^2]$, to model a surface monolayer. Equation (B16) is a standard diffusion-type equation which is solved by Fourier analysis (for any boundary condition) to yield Eqs. (3.16) and (3.17). χ_0 is chosen such that $\Phi_0(0)=\psi_0$, in accordance with the one-dimensional profile Eq. (2.11).

We now determine the function $g(\psi_0,\alpha)$ by using the boundary condition Eq. (B6a)

$$\Phi_2(x,y,z=0)=0\ .$$

Putting $\chi(\bar{x},\bar{y},\bar{z})$ back into Eq. (B12), one obtains after some algebra:

$$\Phi_2(\bar{x},\bar{y},z,\bar{z})=A(\bar{x},\bar{y},\bar{z})\Phi_{0,z}+\xi_\beta\Phi_{0,z}\int_z^\infty\Phi_{0,z'}\int_z^{z'}\frac{d\bar{z}}{(\Phi_{0,\bar{z}})^2}\left[\frac{2/\xi^2}{[1+(\xi_\beta/\xi)(\bar{z}/\xi)]}(\xi_\beta\Phi_{0,z'z'}+\Phi_{0,z'})\right.$$
$$\left.+g(\psi_0,\alpha)\left[\frac{1}{\xi_\beta}\Phi_0-\xi_\beta\Phi_{0,z'z'}\right]\right]dz' \tag{B17}$$

where Φ_0, given by Eq. (3.15), is a function of $\bar{x},\bar{y},z,\bar{z}$. For $\beta>\beta_c$, imposing the boundary condition Eq. (B6a) merely fixes a boundary condition on the function $A(\bar{x},\bar{y},\bar{z})$ at $\bar{z}=0$. The function $A(\bar{x},\bar{y},\bar{z})$ itself is not determined till higher-order terms are considered. However, when $\beta=\beta_c$, $\psi_0=\psi_M(\beta_c)$, and $\Phi_{0,z}=0$ at $\mathbf{r}=\mathbf{0}$. Thus, for $\beta=\beta_c$ the boundary condition on Φ_2 at $\mathbf{r}=\mathbf{0}$ yields the expression:

$$\lim_{z\to0}\Phi_{0,z}\int_z^\infty\Phi_{0,z'}\int_z^{z'}\frac{d\bar{z}}{(\Phi_{0,\bar{z}})^2}\left[\frac{2}{\xi^2}(\xi_{\beta_c}\Phi_{0,z'z'}+\Phi_{0,z'})+g(\psi_0,\alpha)\left[\frac{1}{\xi_{\beta_c}}\Phi_0-\xi_{\beta_c}\Phi_{0,z'z'}\right]\right]dz'=0\ , \tag{B18}$$

where all functions in the integrand are evaluated at $\bar{x}=\bar{y}=\bar{z}=0$ and Φ_0 is taken with $\beta=\beta_c$ [Eq. (3.16)].

Equation (B18) is an equation for the coefficient $g(\psi_0,\alpha)$ which is determined by the ratio of two integrals [similar to Eqs. (A20)–(A22)]. As in Appendix A we expand $\Phi_{0,z}\approx\psi_0+bz^2/2$ for small z.

(i) The numerator was evaluated in Appendix A and the result is

$$N=\frac{2}{\xi^2 b}\int_0^\infty\Phi_{0,z}^2dz\ .$$

(ii) The denominator is:

$$D=\lim_{z\to0}\Phi_{0,z}\int_z^\infty\left[\xi_{\beta_c}\Phi_{0,z'}\Phi_{0,z'z'}-\frac{1}{\xi_{\beta_c}}\Phi_{0,z'}\Phi_0\right]$$
$$\times[H(z')-H(z)]dz'\ , \tag{B19}$$

where $H(z)=\int dz/(\Phi_{0,z})^2$ (see Appendix A). Integrating by parts we obtain:

$$D=\lim_{z\to0}bz\left[\left[\frac{\xi_{\beta_c}}{2}\Phi_{0,z'}^2-\frac{1}{2\xi_{\beta_c}}\Phi_0^2\right][H(z')-H(z)]\right]_z^\infty$$
$$-\lim_{z\to0}bz\int_z^\infty\left[\frac{\xi_{\beta_c}}{2}-\frac{1}{2\xi_{\beta_c}}\frac{\Phi_0^2}{\Phi_{0,z'}^2}\right]dz'\ .$$

The first term vanishes in the limits. The second integral does not diverge for $z'\to\infty$ since the integrand vanishes. The contributions come only from the region $z'\approx0$. The result is

$$D=\frac{1}{2b}\frac{\psi_0^2}{\xi_{\beta_c}}\ .$$

Finally, we find $g(\psi,\alpha)$ as given by Eq. (3.19). Again, implicit in Eq. (3.19) is that Φ_0 is given by Eq. (3.16) with β_c evaluated at $\bar{x}=\bar{y}=\bar{z}=0$.

[1] M. Gavish, R. Popovitz-Biro, M. Lahav, and L. Leiserowitz, Science **250**, 973 (1990).

[2] J. S. Langer, Ann. Phys. (N.Y.) **41**, 108 (1967).

[3] J. S. Langer, Phys. Rev. Lett. **21**, 973 (1968).

[4] J. S. Langer, Ann. Phys. (N.Y.) **54**, 258 (1969).

[5] J. Gunton, M. san Miguel, and P. S. Sahni, in *Phase Transitions and Critical Phenomena,* edited by C. Domb and J. Lebowitz (Academic, New York, 1983), Vol. 8, and references therein.

[6] R. Bar-Ziv and S. A. Safran, Europhys. Lett. **22**, 251

(1993).
[7] J. Lee Kavanau, *Water and Solute-Water Interactions* (Holden-Day, San Francisco, 1964).
[8] M. Elbaum and M. Schick, J. Phys. I (France) **1**, 1665 (1991).
[9] M. Gavish, J.-L. Wang, M. Eisenstein, M. Lahav, and L. Leiserowitz, Science **256**, 815 (1992).
[10] T. V. Ramakrishnan and M. Yussouff, Phys. Rev. B **19**, 2775 (1979).
[11] S. Alexander and J. McTague, Phys. Rev. Lett. **41**, 702 (1978).
[12] A. D. J. Haymet, and D. W. Oxtoby, Chem. Phys. **74**, 2559 (1981); D. W. Oxtoby and A. D. J. Haymet Chem. Phys. **76**, 6262 (1982).
[13] M. Grant and J. D. Gunton, Phys. Rev. B **32**, 7299 (1985).
[14] P. Harrowell and D. W. Oxtoby, Chem. Phys. **80**, 1639 (1984).
[15] Jean-Claude Toledano and Pierre Toledano, *The Landau Theory of Phase Transitions* (World Scientific, Singapore, 1987).
[16] R. Lipowsky, Phys. Rev. Lett. **49**, 1575 (1982).
[17] R. Lipowsky, D. M. Kroll, and K. P. Zia, Phys. Rev. B **27**, 4499 (1983).
[18] R. Lipowsky and W. Speth, Phys. Rev. B **28**, 3983 (1983).
[19] G. Forgacs, R. Lipowsky, and Th. M. Nieuwenhuizen, in *Phase Transitions and Critical Phenomena* (Ref. [5]), Vol. 14.
[20] Donald R. Smith, *Singular Perturbation Theory, An Introduction with Application* (Cambridge University, Cambridge, 1985).
[21] We have in mind a surface domain modeled by $h(x,y) \approx \psi_0 \exp[-(x^2+y^2)]/2L^2$, hence for $x,y < L, h_{xx} \approx -f/L^2$. This will be true for domains described with a single length scale; more complex profiles can be treated in a similar manner.

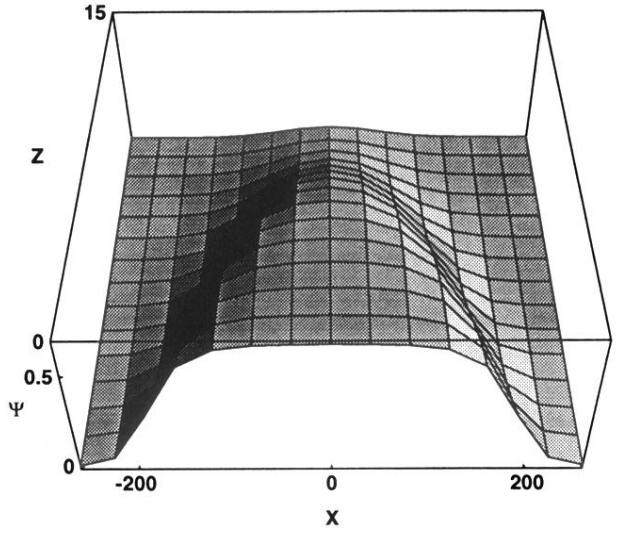

FIG. 7. The shape of Φ_0 from Eq. (3.19) in three dimensions (with $y=0$) at $L=L_c$ with $\psi_0=0.66$ and $\alpha=0.222$.